HAL
open science

Catalytic and thermal characterisations of nanosized PdPt / Al2O3 for hydrogen detection

Thomas Mazingue, Marc Lomello-Tafin, Michelle Passard, Camilo Hernandez-Rodriguez, Laurent Goujon, Jean-Luc Rousset, Franck Morfin, Laithier Jean-François

To cite this version:

Thomas Mazingue, Marc Lomello-Tafin, Michelle Passard, Camilo Hernandez-Rodriguez, Laurent Goujon, et al.. Catalytic and thermal characterisations of nanosized PdPt / Al2O3 for hydrogen detection. Journal of Sensors and Sensor Systems, 2014, Special Issue: Advanced functional materials for environmental monitoring and applications, 3, pp.273-280. 10.5194/jsss-3-273-2014 . hal-01082926

HAL Id: hal-01082926

https://hal.science/hal-01082926v1

Submitted on 14 Nov 2014

HAL is a multi-disciplinary open access archive for the deposit and dissemination of scientific research documents, whether they are published or not. The documents may come from teaching and research institutions in France or abroad, or from public or private research centers.

L'archive ouverte pluridisciplinaire **HAL**, est destinée au dépôt et à la diffusion de documents scientifiques de niveau recherche, publiés ou non, émanant des établissements d'enseignement et de recherche français ou étrangers, des laboratoires publics ou privés.

J. Sens. Sens. Syst., 3, 273–280, 2014
www.j-sens-sens-syst.net/3/273/2014/
doi:10.5194/jsss-3-273-2014
© Author(s) 2014. CC Attribution 3.0 License.

JSSS Journal of Sensors and Sensor Systems Open Access

Catalytic and thermal characterisations of nanosized PdPt / Al_2O_3 for hydrogen detection

T. Mazingue[1], M. Lomello-Tafin[1], M. Passard[1], C. Hernandez-Rodriguez[1], L. Goujon[1], J.-L. Rousset[2], F. Morfin[2], and J.-F. Laithier[3]

[1]Univ. Savoie, SYMME, 74000 Annecy, France
[2]Institut de Recherches sur la Catalyse et l'Environnement de Lyon (IRCELYON, CNRS – University of Lyon), 2 avenue Albert Einstein, 69626 Villeurbanne CEDEX, France
[3]Comelec SA, Rue de la Paix 129 – 2301 La Chaux-de-Fonds, Switzerland

Correspondence to: T. Mazingue (thomas.mazingue@univ-savoie.fr)

Received: 13 June 2014 – Revised: 18 September 2014 – Accepted: 10 October 2014 – Published: 30 October 2014

Abstract. Palladium platinum (PdPt) has been intensively studied these last decades due to high conversion rate in hydrogen oxidation at room temperature with significant exothermic effects. These remarkable properties have been studied by measuring the temperature variations of alumina (Al_2O_3) supported nanosized PdPt nanoparticles exposed to different hydrogen concentrations in dry air. This catalyst is expected to be used as a sensing material for stable and reversible ultrasensitive hydrogen sensors working at room temperature (low power consumption). Structural and gas sensing characterisations and catalytic activity of PdPt / Al_2O_3 systems synthesised by co-impregnation will be presented. Catalytic characterisations show that the system is already active at room temperature and that this activity sharply increases with rise in temperature. Moreover, the increase of the PdPt proportion in the co-impregnation process improves the activity, and very high conversion can be reached even at room temperature. The thermal response (about 3 °C) of only 1 mg of PdPt / Al_2O_3 is reversible, and the time response is about 5 s. The integration of PdPt / Al_2O_3 powder on a flat substrate has been realised by the deposition onto the powder of a thin porous hydrophobic layer of parylene. The possibility of using PdPt in gas sensors will be discussed.

1 Introduction

Hydrogen is a promising non-polluting alternative to fossil fuels as an energy carrier. Its storage for domestic applications remains problematic, since the hydrogen molecule is very small (74×10^{-12} m), inducing a risk of leaks leading to explosion (lower explosion limit LEL = 4 % of hydrogen in the air). There already exist many hydrogen sensors (Meixner and Lampe, 1996), based for example on electrolytic (Kroll and Smorchkov, 1996) or catalytic (Shin et al., 2009; Han et al., 2007) reactions, widely used in industrial plants. But most of these devices need important power supplies (for reaction activation and desorption process), and suffer from drift of measured values and poisoning (Barsan et al., 2007). We propose in this work to use palladium platinum (PdPt) nanoclusters supported by alumina (PdPt / Al_2O_3) for H_2 detection. This bimetallic catalyst has been intensively studied these last decades for numerous remarkable properties, including good conversion rate in hydrogen oxidation at room temperature with high exothermal effects ($\Delta H_{25\,°C,vap} = -241.8\,KJ\,mol^{-1}$; Lide, 2001) and high resistance to poisoning (Rousset et al., 2001; Morfin et al., 2004; Rousset et al., 2001). We present here the PdPt / Al_2O_3 synthesis by co-impregnation, morphology, catalytic activity and gas sensing characterisations. Catalytic characterisations show that conversion starts below room temperature and increases quickly with temperature. The thermal response (about 3 °C) of only 1 mg of PdPt / Al_2O_3 is reversible at room temperature, and the time response is about 5 s. We conclude on the possibility of using PdPt in gas sensors.

2 Experiment

2.1 PdPt / Al_2O_3 synthesis

The PdPt / Al_2O_3 catalysts are prepared by co-impregnation of metallic precursors (Pd and Pt acetyl acetonates) on two Al_2O_3 powders with different grain sizes, crystalline phases and specific surface areas ($\alpha-Al_20_3$: 0.3 µm, 7.7 $m^2\,g^{-1}$, and $\gamma-Al_20_3$: 2.6 µm, 56 $m^2\,g^{-1}$) in a solution of toluene stirred for 24 h. Then the solution is dried (evaporation of the toluene under vacuum at 80 °C for a day). Finally, stages of decomposition (450 °C in Ar), calcination (350 °C in O_2) and reduction (450 °C in H_2) are performed. Three catalysts (A, B and C) have been synthesised on both sizes of alumina, and one with alpha alumina, with different concentrations of Pt and Pd. They all are in the form of a grey powder with a texture similar to flour.

2.2 Sample characterisations

The chemical composition of the catalysts synthesised is determined by ICP-OES (inductively coupled plasma – optic emission spectroscopy). Transmission electron microscopy (TEM) is used to characterise the size and the morphology of the metallic particles.

2.3 Catalytic activity

The oxidation of H_2 by synthesised PdPt / Al_2O_3 samples has then been carried out at atmospheric pressure in a continuous-flow fixed-bed reactor. The experimental set-up is described in detail in Rossignol et al. (2005). The catalyst (6 mg) is exposed to a reactive mixture consisting of 0.5 %H_2 + 10 %O_2 in He at a flow rate of 50 mL min^{-1}. The gas mixture is analysed at the output of the reactor and compared to the initial composition by a gas chromatograph Varian-Micro GC (CP2003) equipped with thermal conductivity detectors. The reactor is immersed in an isothermal water bath whose temperature was set between 0 and 70 °C. Catalytic conversion is measured after 20 min of stabilisation. A thermocouple located inside the catalytic bed is used to measure the catalyst temperature.

2.4 Gas sensitivity characterisations

The principle of the gas sensitivity measurement is to follow with an IR camera the temperature variation of PdPt / Al_2O_3 powder due to the exothermicity associated with the oxidation of H_2. This will provide a relation between the different H_2 concentrations and the variations of the temperature. This thermal response is considered as the gas sensitivity. The PdPt / Al_2O_3 samples are placed on a clean substrate in the gas chamber. The experimental set-up is described in more details in Mazingue et al. (2012). Before proceeding with the oxidation of H_2, a flow of dry air is sent into the gas chamber for at least 10 min to evacuate eventual impurities and undesired uncontrolled humidity. The experimental protocol is then started with three alternate sequences of 30 s of dry air and a given concentration of H_2 (from 200 to 4000 ppm) in dry air under a flow rate of 500 mL min^{-1}. The repeatability and the linearity of the response can thus be evaluated. The thermal response is measured with an IR camera CEDIP JADE III MW under ALTAIR software, through a sapphire window above the gas chamber. The principle is to use each camera pixel as a small thermometer. A differential thermal average measurement is performed between a surface occupied by a determined mass of nanopowder and a free surface of the same area separated by a small distance on the same substrate. All electronic devices and pneumatic valves are monitored by a LabVIEW application, via a CompactRIO/FPGA.

Table 1. Physical and chemical characterisations of PdPt / Al_2O_3 synthesised by co-impregnation.

Catalyst	A	B	C
Support	γ-Al_2O_3	α-Al_2O_3	γ-Al_2O_3
Pd (%wt)	0.7	0.6	5.4
Pt (%wt)	2.2	0.7	15.4
Φ (nm)	3.8	6.2	4–10

3 Results and discussions

Catalysts A and B have been first synthesised as described above, respectively, on gamma and alpha alumina. Their chemical compositions are given in Table 1. It has been observed that much of platinum (70 %) introduced into the impregnating solution is lost during the synthesis of the catalyst on alpha alumina (sample B). This loss is much less pronounced for the palladium, and it is not present on the gamma alumina (sample A), which has a much larger specific surface area. The metallic proportion is therefore much higher for A (3.3 %wt) compared to B (0.9 %wt for B). As the efficiency of the catalyst increases with the metallic proportion, it has been chosen to synthesise sample C with higher quantities of metallic precursors on γ-Al_2O_3. This leads to powders with metallic concentrations up to 20.8 %wt for sample C. Figure 1 shows that the morphology of the catalyst remains in the form of nanoparticles deposited on alumina, independently of the metallic concentration.

Figure 2 shows that, without prior activation (a first cycle of heating and cooling), the catalytic conversion at room temperature is about 83 % for A but only 18 % for B. Full H_2 conversion is reached at about 60 °C for A and B, but A presents higher conversion rates for lower temperature. This can be explained by the greater amount of metal in the powder in A. Concerning sample C, 100 % of the H_2 is converted at room temperature. This value falls to about 68 % at 5 °C.

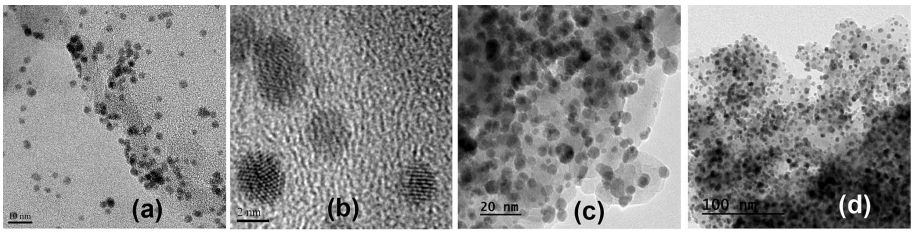

Figure 1. TEM micrographs of catalyst A: **(a)** and **(b)**; catalyst C: **(c)** and **(d)**.

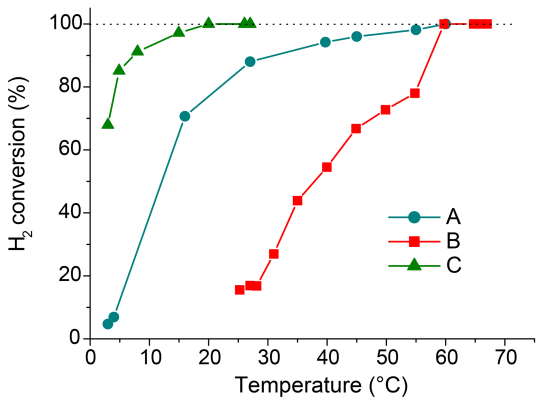

Figure 2. Dependence of H_2 conversion over PdPt / Al_2O_3 versus temperature in a mixture of 0.5 %H_2 +10 %O_2 in He for 5.5 mg of synthesised catalysts A, B and C.

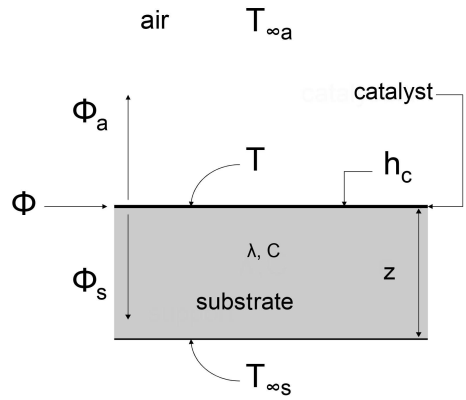

Figure 3. Modelling of the thermal problem.

The samples A and C exhibit very good activity even at room temperature and seem to be good candidates for easy integration into a transducing component, especially catalyst C. Considering these last results, only samples A and C have been taken into account for gas sensitivity characterisations.

We developed a simplified model to explain the thermal response of the catalyst. We consider that a mass m_c of catalyst with a negligible thickness is deposited on a surface S on a substrate with a mass m_s, a thickness z, a thermal conductivity λ and heat capacity C as shown in Fig. 3. The surrounding air temperature is $T_{\infty a}$ above the catalyst. A temperature $T_{\infty s}$ is imposed on the rear side of the substrate. We neglect at the moment the heat exchanges by radiation compared to those by convection ($h_r \ll h_c$). The experiment consists in measuring the temperature T at the surface of the catalyst. T is supposed to be also the temperature on the rear side of the catalyst.

The heat flux to which the system is subjected is as follows:

- $\Delta\Phi = m_s C \frac{\partial T}{\partial t}$ the variation of heat exchange of the system
- Φ the flux created at the surface of the catalyst during the catalytic reaction with the gas
- $\Phi_a = h_c S(T - T_{\infty a})$ the heat exchange with the surrounding air
- $\Phi_s = \lambda S/z(T - T_{\infty s})$ the heat exchange with the substrate.

The flow balance shows that the power variation of the system is equal to the power produced by the catalyst, minus those transferred to the environment, or $\Delta\Phi = \Phi - (\Phi_a + \Phi_s)$, which can also be written as follows:

$$m_s C \frac{\partial T}{\partial t} = \Phi - \left[h_c S(T - T_{\infty a}) + \lambda S/z(T - T_{\infty s})\right]. \quad (1)$$

This can be written in a reduced form:

$$\frac{\partial T}{\partial t} + \frac{T}{\tau} = \frac{T_f}{\tau}, \quad (2)$$

where T_f is the temperature reached by the catalyst once the thermal equilibrium established after a characteristic time τ. Those two last physical quantities are defined as follows:

$$\tau = \frac{m_s C/S}{h_c + \lambda/z}, \quad (3)$$

$$T_f = \frac{\Phi/S + h_c T_{\infty a} + (\lambda/z) T_{\infty s}}{h_c + \lambda/z}. \quad (4)$$

In absence of the target gas, no catalytic reaction occurs, $\Phi = 0$, and the temperature of the catalyst remains constant

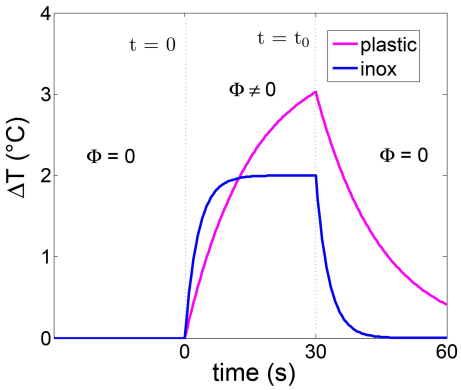

Figure 4. Modelling of the thermal response for a pulse of a given concentration of target gas for a plastic substrate ($\lambda_{plastic} = 0.15\,W\,m^{-1}\,K^{-1}$, $C_{plastic} = 1800\,J\,K^{-1}\,kg^{-1}$, pink curve) and an inox substrate ($\lambda_{inox} = 16\,W\,m^{-1}\,K^{-1}$, $C_{inox} = 502\,J\,K^{-1}\,kg^{-1}$, blue curve).

with temperature:

$$T_0 = \frac{h_c T_{\infty a} + (\lambda/z) T_{\infty s}}{h + \lambda/z}. \quad (5)$$

The resolution Eq. (1) describes the increase of the temperature as soon as the reaction takes place:

$$T(t) = (T_0 - T_f)e^{-t/\tau} + T_f. \quad (6)$$

The elevation of temperature is then

$$T_f - T_0 = \Delta T = \frac{\Phi/S}{h_c + \lambda/z}. \quad (7)$$

We consider now that, at $t < t_0$, the presence of the target gas has stabilised the temperature of the catalyst at $T = T_f$ thanks to $\Phi \neq 0$. At $t = t_0$, the gas inlet is suddenly cut off and Φ becomes zero. By injecting these conditions in Eq. (1), the expression of the temperature becomes, for $t > t_0$,

$$T(t) = (T_f - T_0)e^{-(t-t_0)/\tau} + T_0. \quad (8)$$

This very simplified model gives us important information:

1. ΔT depends on Φ, the thermal flux due to the catalytic reaction. Φ is directly linked to the concentration of the gas in the incoming air flow, and is therefore supposed to remain constant in the experimental conditions. ΔT increases as expected with $1/\lambda$ (homogenous to the thermal resistance) because a low substrate thermal conductivity prevents the heat from escaping on this side of the catalyst.

2. τ does not depend on Φ and therefore on gas concentration.

3. For a given value of Φ, the response time depends on the substrate physical properties. τ increases with the mass m and the heat capacity C of the substrate, and decreases with its thermal conduction λ.

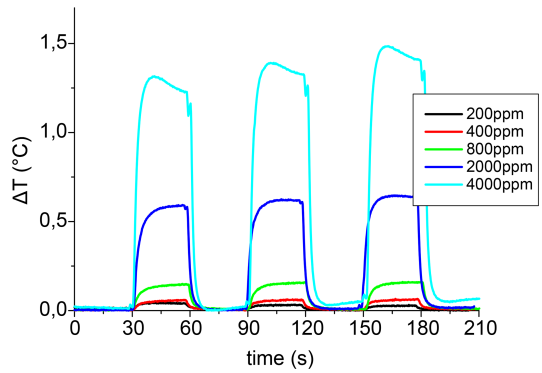

Figure 5. Gas sensitivity of catalyst A exposed to different H_2 concentrations in dry air at room temperature.

This means that the choice of the material used for the substrate is essential. A maximal value of ΔT obtained with a substrate with a low λ will induce a long response time. A compromise has to be found to get a good thermal response, stabilised as quickly as possible. Figure 4 shows the trends of the thermal response according to the model with two different material substrates: inox ($\lambda_{inox} = 16\,W\,m^{-1}\,K^{-1}$, $C_{inox} = 502\,J\,K^{-1}\,kg^{-1}$) and a plastic (polypropylene, $\lambda_{PP} = 0.15\,W\,m^{-1}\,K^{-1}$, $C_{PP} = 1800\,J\,K^{-1}\,kg^{-1}$). The shape is qualitative as physical data such as h_c or S are unknown. The influence of λ and C is clearly visible on ΔT and τ: in the case of an inox substrate (high thermal conductivity), the time response is low and the thermal equilibrium is quickly reached. In case of a plastic substrate, the response time is much longer and the temperature becomes higher, but the thermal equilibrium is not reached at the end of the H_2 exposure. However, the limits of the model are clearly highlighted by the absence of dependence of the thermal response ΔT with the mass m_c of the deposited catalyst. We neglect here the fact that the thermal contact between the catalyst and the substrate is far from perfect, and therefore that the temperature distribution in the catalytic layer is complex. Anyhow, this simplified model fits properly with the measurements, as seen in next paragraph.

Figure 5 shows the thermal response of 1 mg of sample A deposited onto an inox substrate under dry air mixtures with different concentrations of H_2 at room temperature. In accordance with the model described above, we observe that the catalyst exhibits a first-order response when exposed to H_2. Sample A presents a pronounced sensitivity to H_2 at room temperature: elevation of about 0.6 °C for 2000 ppm and 1.2 °C for 4000 ppm. The thermal response is rather fast (about 5 s), and we can note that the response time is not dependent on H_2 concentration, as predicted by our model. The thermal response is also reversible (quick return to the baseline in the absence of H_2), at room temperature. This means that no additional energy is needed to desorb H_2 on active sites where oxidation occurs. These results have to be

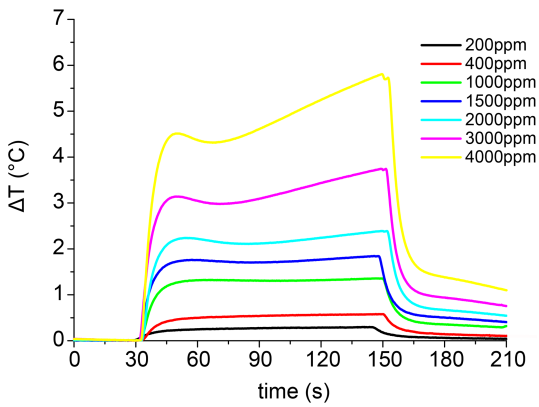

Figure 6. Stability of the thermal response of sample C to different concentrations of H_2 in dry air for 120 s.

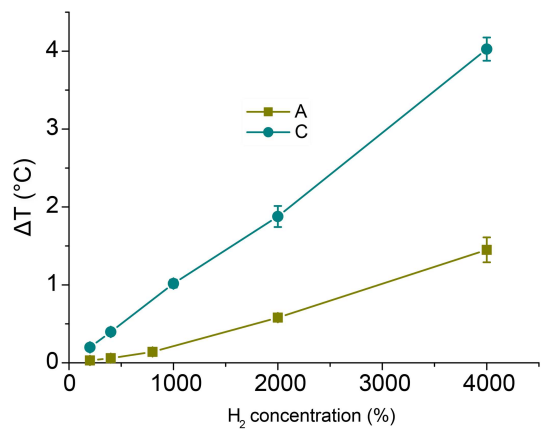

Figure 7. Linear response of the sensitivity of catalysts A and C.

compared with the 0.1 °C temperature variation obtained for the same mass of Au / CeO_2 under 500 ppm CO diluted in dry air (Mazingue et al., 2012). The shape of the plateau for an exposition of the catalyst to 4000 ppm shows that it can take time to get the thermal equilibrium. Indeed, the heat produced by the catalytic reaction increases the conversion rate of H_2, as observed in Fig. 2. With our model, we can deduce that Φ is then reaching a greater value, inducing a subsequent rise of temperature. This phenomenon is repeated as long as the external thermal conditions do not allow the thermal equilibrium for H_2 concentrations above 1500 ppm, as shown in Fig. 6. The stability of the thermal response decreases therefore when the H_2 concentration increases. However, the derivative of the expression of the temperature (Eq. 6) leads to the following formula:

$$\frac{\mathrm{d}T}{\mathrm{d}t} = \frac{\Delta T}{\tau} \exp^{-t/\tau} . \tag{9}$$

The slope of the curve at $t = 0$ is given by

$$\frac{\Delta T}{\tau} = \frac{\Phi}{m_s C} . \tag{10}$$

Since Φ is directly linked to the gas concentration, it is possible, by an adapted signal treatment on the derivative of the signal before the thermal equilibrium, to get a piece of information on the gas concentration.

The same tests have been performed with sample C and identical experimental conditions, giving the same kind of results but with higher thermal responses. Figure 7 gives a comparison between the performances of catalyst A and C: both exhibit linear and repeatable responses. Catalyst C is clearly the best candidate to be used as sensitive material in the H_2 sensor. The range of temperature variations can be easily detected by many kind of transducers, such as surface acoustic waves (SAWs) (Stelzer et al., 2008). These results also are promising for H_2 detection by optical means (Mazingue et al., 2007) since recent studies showed that temperature variations in the °C range can be monitored (Wood et al., 2013).

The integration of the catalyst onto a transducer has to preserve the catalytic properties and supply a mechanical support. However, most of the used methods of deposition led to a loss of activity. Chemical methods such as dispersion into a porous sol-gel matrix induce an encapsulation of the catalyst. Incorporation of PdPt nanoclusters into thin mesoporous film such as TiO_2 or SiO_2 by co-impregnation (with the technique described above) gives a too high dispersion of the catalyst to allow a measurable thermal response. Physical methods such as chemical vapour deposition or pulsed laser deposition gave very flat catalyst layers, with limited reactive surface and therefore a low catalytic activity. We found an alternative by coating the catalyst with a thin layer of parylene, maintaining the powder onto a substrate without killing its catalytic activity. Parylene is a high-tech, ultrathin, transparent coating that is physically and chemically neutral, inert, biocompatible, and biostable. It insulates and protects, and can easily and accurately be applied in any thickness, from 50 nm to 100 µm. It is completely uniform, without pinholes, and suitable for application to very small technical components (protection against moisture, aggressive environment) and/or as an electrical insulator, resistance to all solvents, acids, and bases (Trantidou et al., 2013). The deposition process occurs in vacuum at room temperature. The coating ensures a hydrophobic protection to the catalyst, but is permeable enough to H_2.

A quantity of 1 mg of sample A deposited onto an oxidised Si wafer has been coated by different thicknesses of parylene (determined after deposition by interferometric measurements) and been exposed to increasing concentration of H_2 in dry air. Figure 8 shows that all the samples present a thermal response, but ΔT decreases with parylene thickness. This is not surprising, considering that parylene is a barrier for H_2 molecules to reach active sites of the catalyst. However, for a parylene thickness of 700 nm, a ΔT of 1 °C can

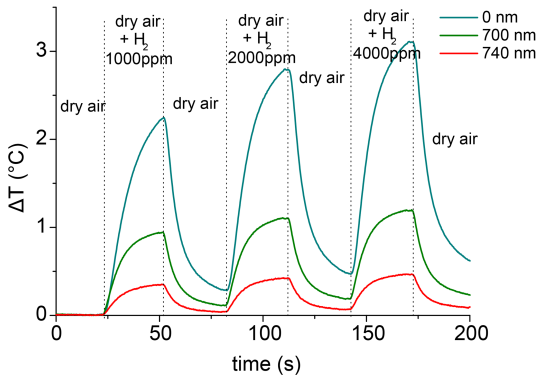

Figure 8. Thermal response of catalyst A coated by different thicknesses of parylene.

still be observed for a concentration of 4000 ppm. We can also notice that the shape of the thermal response is different from previous experiments because the substrate was in this case an oxidised Si wafer, with much lower thermal conductivity. As predicted by our simplified model and depicted in Fig. 6, the resulting thermal response is characterised by a higher ΔT and longer response time τ. A cumulative drift is then observed. This can be explained by the fact that the thermal equilibria cannot occur with exposure times as short as 30 s. We would observe no drift with exposure times much longer than response times. Moreover, the curves pictured in Fig. 8 have been performed after several tests according to the protocol described in the experimental part. During the first exposition of H_2, the samples coated with parylene gave a thermal response such as the ones in Fig. 8, whereas the uncoated sample exhibited no temperature rise. This can be explained by the fact that uncoated PdPt / Al_2O_3 must get rid of adsorbed water on active sites so that catalytic reaction can occur. This happens after several cycles of dry air and H_2 exposition, which would be problematic for a gas sensing application (hygrometry dependence). Coated catalysts do not have this problem, as the parylene deposition is performed in a vacuum at room temperature, inducing a water desorption of the active sites. Once coated, the latter are water free and interact directly with H_2 molecules, as explained in Appendix A. Parylene coating seems therefore to present all the required properties for efficient integration of PdPt / Al_2O_3 nanopowders on a transducer for gas sensing applications.

4 Conclusions

Catalytic activity and thermal response of PdPt / Al_2O_3 nanostructured catalysts to H_2 synthesised by the co-impregnation method have been characterised. It has been observed that the nature of the alumina support is relevant for the optimisation of the metallic proportion of the final system, leading to a greater catalytic activity. γ-PdPt / Al_2O_3 will therefore be preferred to α-PdPt / Al_2O_3 for gas sensing applications because of its higher specific surface area. Full H_2 conversion at room temperature can be reached by increasing the proportions of the metallic precursors in the synthesis process. The H_2 sensitivity tests showed that the thermal response of the catalysts is reversible with a time response of 5 s, at room temperature, and fits with a simplified model we developed to explain the shape of the curves. The temperature rise is in the °C range for only 1 mg of catalyst, and concentrations of H_2 in dry air ranging from 200 to 4000 ppm. However, the stability of thermal response is problematic for H_2 concentrations above 1500 ppm because of the establishment of the thermal equilibrium is harder to reach. Nevertheless, an integration method has been investigated by coating the catalyst with a parylene thin film. Sensitivity tests show that the thermal response decreases with the thickness of the coating, but still exhibits significant temperature rise (in the °C range). All these results are promising for integration of PdPt / Al_2O_3 nanostructured catalyst onto different transducers for fast-response, reversible, and room-temperature working gas-sensing systems. Alternative devices such as photonic (Bragg gratings and multimode interference couplers) or SAW transducers are under study to develop reversible remote controlled and passive components for the detection of H_2, working in a large range of temperatures in harsh environments, with no need for embedded energy.

Appendix A: Water permeability of the parylene

We presented in our article the possibility of using PdPt nanoclusters supported by alumina (PdPt / Al_2O_3) for H_2 detection. This bimetallic system is a catalyst for the following exothermal reaction (Munakata et al., 2011) :

$$H_2 + \frac{1}{2}O_2 \overset{\text{PdPt}}{\rightarrow} H_2O. \tag{A1}$$

The heat generated during the reaction leads to a temperature rise of the catalyst that is directly linked to the H_2 concentration. The catalyst is maintained on a substrate with a thin film of parylene, a transparent and hydrophobic polymer. The aim of the following text is to show that the formed water during the catalytic reaction is in a gaseous state and induces no poisoning on the active sites of the catalyst.

The transmission of vapour through a membrane is measured at a temperature of 38 °C and 100 % of relative humidity, according to the norm ASTM F1249-06. The unit of measurement is $\mathrm{g\,mm\,m^{-2}\,d^{-1}}$. This physical quantity can be considered as the mass of water vapour passing through a membrane 1 mm thick, per area unit ($\mathrm{m^2}$) and per time unit (day).

As the molar mass of water is $M_{H_2} = 18\,\mathrm{g\,mol^{-1}}$, we have, in a mass $m = 1\,\mathrm{g}$ of water, $n = m/M_{H_2} = 0.056\,\mathrm{mol}$. As the molar volume is $V_M = 24.79\,\mathrm{L\,mol^{-1}}$ at $T = 25\,°\mathrm{C}$[1], 1 g of water vapour occupies a volume of $V_M \times n = 24.79 \times 0.056 = 1.377\,\mathrm{L} = 1377\,\mathrm{cm^3}$.

The permeability of the parylene layer we used in this work is $0.1\,\mathrm{g\,mm\,m^{-2}\,d^{-1}}$,[2]. The parylene thickness was $740\,\mathrm{nm} = 740 \times 10^{-6}\,\mathrm{mm}$. The permeability of the parylene film related to this thickness is therefore $135\,\mathrm{g\,m^{-2}\,d^{-1}}$ or $1.86 \times 10^5\,\mathrm{cm^3\,m^{-2}\,d^{-1}}$ (the molar volume of ideal gas is $V_M = 24.79\,\mathrm{L\,mol^{-1}}$ at $T = 25\,°\mathrm{C}$[3]).

The gas permeability of a membrane is measured differently than for water. The used method is performed according to the norm ASTM D1434 F3985-05, at a temperature of 25 °C. The unit of measurement is the $\mathrm{cm^3\,mm\,m^{-2}\,d^{-1}\,bar^{-1}}$. This physical quantity can be considered as the gas volume passing through a membrane 1 mm thick, per area unit ($\mathrm{m^2}$), per pressure unit (bar) and per time unit (day).

The parylene we used in our work presents a H_2 permeability of $42\,\mathrm{cm^3\,mm\,m^{-2}\,d^{-1}\,bar^{-1}}$,[2]. We had a parylene thickness of $740 \times 10^{-6}\,\mathrm{mm}$. The permeability of the parylene film related to this thickness is therefore $42/740 \times 10^{-6} = 5.6 \times 10^4\,\mathrm{cm^3\,m^{-2}\,d^{-1}\,bar^{-1}}$.

Since the gas mixture is injected in the test chamber at a pressure of 1 bar and a H_2 concentration of 4000 ppm, the partial H_2 pressure is 4×10^{-3} bar. The H_2 permeability of a thickness of 740 nm of parylene at this pressure is then $56 \times 10^3 \times 4 \times 10^{-3} = 227\,\mathrm{cm^3\,m^{-2}\,d^{-1}}$. The parylene is therefore much more permeable to water vapour than to hydrogen.

In our conditions, the H_2 partial pressure $P_{H_2} = 4\,\mathrm{mbar}$ is much lower than the saturated vapour pressure of water $P^0_{H_2O,25\,°C} = 31.7\,\mathrm{mbar}$[4]. Hence, even if we consider that the totality of the H_2 passes through the parylene and is oxidised into H_2O, the formed water will never condense since its partial pressure is much lower than the saturated vapour pressure. Moreover, we showed that the permeability of the parylene would be much higher for water vapour than for H_2. That means that vapour will be removed from the catalyst side faster than H_2 will be provided by our experiment. We can conclude that the formed water will not accumulate on the surface of the catalyst and thus will not poison it since it will stay in a gaseous state and will be removed quickly in the surrounding atmosphere.

[1] http://en.wikipedia.org/wiki/Standard_conditions_for_temperature_and_pressure

[2] http://www.comelec.ch/en/parylene_tableaux.php

[3] http://en.wikipedia.org/wiki/Standard_conditions_for_temperature_and_pressure

[4] http://www.thermexcel.com/english/tables/eau_atm.htm

Acknowledgements. Part of this work is funded by the French National Agency of the Research (ANR) within the framework of the 2009 P3N program (PEPS project) and Gravit Innovation Grenoble Alpes.

Edited by: A. Romano-Rodriguez
Reviewed by: two anonymous referees

References

Barsan, N., Koziej, D., and Weimar, U.: Metal oxide-based gas sensor research: How to?, Sens. Actuat. B-Chem., 121 , 18–35, 2007.

Han, C.-H., Hong, D.-W., Han, S.-D., Gwak, J., and Singh, K. C.: Catalytic combustion type hydrogen gas sensor using TiO_2 and UV-LED, Sens. Actuat. B-Chem., 125, 224–228, 2007.

Kroll, A. and Smorchkov, V.: Electrochemical solid-state microsensor for hydrogen determination, Sens. Actuat. B-Chem., 34, 462–465, 1996.

Lide, D. R.: Standard Thermodynamic Properties of Chemical Substances, CRC Handbook of Chemistry and Physics, 83rd Edn. CRC Press, Boca Raton, FL, 5-.4–5.60, 2001.

Mazingue, T., Kribich, R., Etienne, P., and Moreau, Y.: Simulations of refractive index variation in a multimode interference coupler: Application to gas sensing, Opt. Commun., 278, 312–316, 2007.

Mazingue, T., Lomello-Tafin, M., Gautier, G., Passard, M., Goujon, L., Hernandez-Rodriguez, C., Rousset, J.-L., and Morfin, F.: Characterizations of gold nanostructured catalysts for gas sensing applications, Proc. of AES-ATEMA, Advanced Engineering Solutions – Advances and Trends in Engineering Materials and their Applications 11th International Conference, Toronto, Canada, 6–10 August, 205–212, 2012.

Meixner, H. and Lampe, U.: Metal oxide sensors, Sens. Actuat. B-Chem., 33, 198–202, 1996.

Morfin, F., Sabroux, J.-C., and Renouprez, A.: Catalytic combustion of hydrogen for mitigating hydrogen risk in case of a severe accident in a nuclear power plant: study of catalysts poisoning in a representative atmosphere, Appl. Catal. B-Environ., 47, 47–58, 2004.

Munakata, K., Wajima, T., Hara, K., Wada, K., Shinozaki, Y., Katekari, K., Mochizuki, K., Tanaka, M., and Uda, T.: Oxidation of hydrogen isotopes over honeycomb catalysts, J. Nucl. Mat., 417, 1170–1174, 2011.

Rossignol, C., Arrii, S., Morfin, F., Piccolo, L., Caps, V., and Rousset, J.-L.: Selective oxidation of CO over model gold-based catalysts in the presence of H_2, J. Catal., 230, 476–483, 2005.

Rousset, J.-L., Stievano, L., Cadete Santos Aires, F. J., Geantet, C., Renouprez, A., and Pellarin, M.: Hydrogenation of Toluene over γ-Al_2O_3-Supported Pt, Pd, and Pd-Pt Model Catalysts Obtained by Laser Vaporization of Bulk Metals, J. Catal., 197, 335–343, 2001.

Rousset, J.-L., Stievano, L., Cadete Santos Aires, F. J., Geantet, C., Renouprez, A., and Pellarin, M.: Hydrogenation of Tetralin in the Presence of Sulfur over γ-Al_2O_3-Supported Pt, Pd, and Pd-Pt Model Catalysts, J. Catal., 202, 163–168, 2001.

Shin, W., Nishibori, M., Ohashi, M., Izu, N., Itoh, T., and Matsubara, I.: Ceramic Catalyst Combustors of Pt-Loaded-Alumina on Microdevices, J. Ceram. Soc. Japan, 117, 659–6655, 2009.

Stelzer, A., Scheiblhofer, S., Schuster, S., and Teichmann, R.: Wireless sensor marking and temperature measurement with SAW-identification tags, Measurement, 41, 579–588, 2008.

Trantidou, T., Payne, D. J., Tsiligkiridis, V., Chang, Y.-C., Toumazou, C., and Prodromakis, T.: The dual role of parylene C in chemical sensing: Acting as an encapsulant and as a sensing membrane for pH monitoring applications, Sens. Actuat. B-Chem., 186, 1–8, 2013.

Wood, T., Le Rouzo, J., Flory, F., Kribich, R., Maulion, G., Signoret, P., Coudray, P., and Mazingue, T.: Study of the influence of temperature on the optical response of interferometric detector systems, Sens. Actuat. A-Phys., 203, 37–46, 2013.